Supplementary information

Hypoxia-induced p53 modulates both apoptosis and radiosensitivity via AKT

Katarzyna B. Leszczynska, Iosifina P. Foskolou, Aswin G. Abraham, Selvakumar Anbalagan, Céline Tellier, Syed Haider, Paul N. Span, Eric E. O'Neill, Francesca M. Buffa and Ester M. Hammond

Contents

Supplementary material and methods

Tissue culture

RKO and HCT116 (colorectal carcinoma, from ATCC), H1299 (non-small cell lung carcinoma, from ATCC), OE21 (esophageal squamous carcinoma, from ECACC), PSN1 (pancreatic adenocarcinoma, a gift from Thomas Brunner, University of Oxford, UK), WI38 (lung fibroblasts, from ATCC) cells were cultured in DMEM with 10% FBS. HCT116 p53$^{+/+}$ and p53$^{-/-}$ cell lines were a gift from Prof Vogelstein (Johns Hopkins University, Baltimore, USA). Mouse embryonic stem cells (CCE line) from Prof Robertson (University of Oxford, UK) were cultured on gelatinized dishes in DMEM medium containing 15% FBS, 1 mM sodium pyruvate, 0.1 mM β-mercaptoethanol, 2 mM L-glutamine, MEM non-essential amino acids, 0.25 U/ml penicillin, 0.25 µg/ml streptomycin, and 1000 U/ml leukemia inhibitory factor (ESGRO®, Millipore). THP-1 (acute monocytic leukemia cell line, from ATCC) were cultured in RPMI medium supplemented with 10% FBS. Lipofectamine Ltx (Invitrogen) was used for plasmid transfections. 5xHRE-driven human p53 constructs (wt p53, p53^{175}) were described (1). 5xHRE-p53^{23,24,53,54}, 5xHRE-p53^{K120R}, 5xHRE-p53^{K164R}, 5xHRE-p53$^{K120/164R}$ were generated by site-directed mutagenesis. The human PHLDA3 sequence was amplified from pDsRed-C1-PHLDA3 kindly provided by Dr Ohki (National Cancer Center Research Institute, Tokyo, Japan) (2) and cloned into pGLS3-5xHRE.

Meta-analysis

A p53 signature from (3) was used to predict p53 status in cancer patients from datatsets (GSE6532KI, GSE6532GUY, GSE6532OXF, GSE9195, GSE1456 and GSE2034) analyzed in Supplemental Figure 6.

Oncomine datasets

The datasets showing a significantly correlation for patients prognosis and collective expression of hypoxia-inducible, p53-dependent group of genes (*PHLDA3, INPP5D, SULF2, BTG2* and *CYFIP2,*) in the Oncomine analysis and showed in Fig. 7A were as follows: (1) Ductal Breast Carcinoma Epithelia (Boersma Breast), (2) & (3) Invasive Ductal Breast Carcinoma (Curtis Breast), (4) Invasive Lobular Breast Carcinoma (Desmedt Breast), (5) Breast Carcinoma (Kao Breast), (6) Breast Carcinoma (Bos Breast), (7) & (8) Lung Adenocarcinoma (DirectorsChallenge Lung), (9) Lung Adenocarcinoma (Garber Lung), (10) & (11) Diffuse Gastric Adenocarcinoma (Forster Gastric), (12) & (13) Mixed Cell Uveal Melanoma (Laurent Melanoma), (14) & (15) Monophasic Synovial Sarcoma (Nakayama Sarcoma 2), (16) Ovarian Serous Adenocarcinoma (Tothill Ovarian), (17) Colon Adenocarcinoma (Jorissen Colorectal 3).

siRNA sequences

PHLDA3-si1 (sense 5'-CUGGAUGGUCCCAGACUCU -3'dTdT),

PHLDA3-si2 (sense 5'-CAGCUUCGUUGUUCCCUCU -3'dTdT),

INPP5D-si1 (sense 5'-GGAAACUGAUCAUUAAGAA -3'dTdT),

INPP5D-si2 (sense 5'-CAGAAAGCGACAGGGAUGA -3'dTdT), all from Sigma-Aldrich;

p53 (sense 5'-GUAAUCUACUGGGACGGAA-3'dTdT) (Ambion /Life Technologies);

negative control siRNA (Scr; #1027310, Qiagen)

qPCR primers

Human gene primers (5'-3'):

18S F: AGTCCCTGCCCTTTGTACACA;

18S R: GATCCGAGGGCCTCACTAAAC;

INPP5D F1: GAGAGGAGGGAGCAGAAGGT;

INPP5D F4: CGCCCACTAATCCTTGATGT;

INPP5D F4a: GAAGACAGGGTCCAGCAGTC;

INPP5D F5: GTGACCCATCTGCAATACCC;

INPP5D R1: GCTTTCTGCTTGGTGTAGGC;

INPP5D R4: GCTTGGACACCATGTTGATG;

PHLDA3 F: GCGCCACATCTACTTCACG;

PHLDA3 R: CACAAGCCAGAGGGAACAAC;

SULF2 F: GACCCCTACCAGCTGATGAA;

SULF2 R: ATAGGCAGTGCCAAGGAAGA;

BTG2 F: TGGGCTTAGGGAACCATCTCT;

BTG2 R: TTCAGCCAAGGAATACATGCAA;

CYFIP2 F: GGTCATGGAGGAACTGCTAA;

CYFIP2 R: TCTTGGGCATCACCTCTATC;

KANK3 F: AGGCAGGAAGAGGAGGACAT;

KANK3 R: ATTCACATCAGCCCCACAC;

GLUT1 F: ATACTCATGACCATCGCGCTAG;

GLUT1 R: AAAGAAGGCCACAAAGCCAAAG;

ABHD4 F: TCACCCACTCTGTCCTTTCC;

ABHD4 R: GTGCAATCCCTTCACATCCT;

CRIP2 F: TAGGCTACAGCGGCTCTCAT;

CRIP2 R: GGGCAGACACACCAGAGACT;

CTSF F: GCCTGTCCGTCTTTGTCAAT;

CTSF R: TGGCTTGCTTCATCTTGTTG;

MGMT F: GGCACCGCTGTATTAAAGGA;

MGMT R: CAAGGGCAGCGTTAGAGAAG;

SIDT2 F: GCCAAATTGCTGCTTTCTTC;

SIDT2 R: TCCCTTCCATCCTTCCTCTT;

TTC28 F: ACCACGGCACAATAAGAAGG

TTC28 R: AGCCATTTCCAGAAGGAAGC;

DEF6 F: AGTCTCCAAGTCCCAGCTCA;

DEF6 R: TGCCCGATAGTTCTTCTTGG;

ARAP2 F: TTGGCCTTGGTCTTTTCATC;

ARAP2 R: ACAGTCGGGTTCCTTCCTTT;

RGS12 F: CAGAAAGGTGTGCCAGTGAA;

RGS12 R: ACTCCTCTGCTTCGTCCAAA;

NDRG4 F: ATGCTTTCCATCCACTCACC;

NDRG4 R: TCACTGCTCTCTCCCGTTTT;

POLK F: AGGGCATTGCTTTCTCTCCT;

POLK R: CTCTCTCCATCCCTCGTCAG;

ERCC5 F: CCCCCTGAAGTAAAGCATGA;

ERCC5 R: CGGATGTGTCCTGAATGTTG;

BAX F: TGTCGCCCTTTTCTACTTTGC;

BAX R: GTCCAGCCCCATGATGGTTCT;

RPS29 F: GCACTGCTGAGAGCAAGATG;

RPS29 R: ATAGGCAGTGCCAAGGAAGA;

INPPL1 F: CAAGCCAGAGCACGAGAAC;

INPPL1 R: CCGCAGGATGTCCAAGTAGT.

Mouse gene primers (5'-3'):

Rn18s F: GACTCAACACGGGAAACCTC;

Rn18s R: GACAAATCGCTCCACCAACT;

Inpp5d F: TTGAACTTTACCTTGAACCTCTGC;

Inpp5d R: GGAACGCCTGTTGGTAGATT;

Glut-1 F: ATCCCATCCACCACACTCAC;

Glut-1 R: GAGAAGCCCATAAGCACAGC;

ChIP primers

INPP5D_ChIP_F: GCCTTGATCTTTGCCCGGG

INPP5D_ChIP_R: TCCGGATGACTTCTCTGGGG

PHLDA3_ChIP_F: GGCGCAGGAGGCGAGCGGCGGAACA

PHLDA3_ChIP_R: CGCTCCTCCGCTCTACCCCAGCTGG

SULF2_ChIP_F: TCCCAAATCAGGTCCAAATC

SULF2_ChIP_R: GAGGAGGACAGCATAGCAGTG

CYFIP2_ChIP_F: CCACCGCTGGGCAGATAATTG

CYFIP2_ChIP_R: AAGGATCCGACAGAAGATGCAACTGG

KANK3_ChIP_F: TCCACACACAAGGGCATCAA

KANK3_ChIP_R: AAACATGGCCAAGTTTGCCC

The following INPP5D CHIP primer sequences were used to map p53 binding to RE

described in (4):

INPP5D-A_ChIP_F: GAAGTGCAGTGGCAAGATCA

INPP5D-A_ChIP_R: GGGAACCCTGCCTCTACAA

INPP5D-B_ChIP_F: GCGACCTCAAAAGGACTGAG

INPP5D-B_ChIP_R: CACCAGCTCACAAAGATGTCA

References

1. Hammond EM, Mandell DJ, Salim A, Krieg AJ, Johnson TM, Shirazi HA, Attardi LD, and Giaccia AJ. Genome-wide analysis of p53 under hypoxic conditions. *Mol Cell Biol.* 2006;26(9):3492-504.
2. Kawase T, Ohki R, Shibata T, Tsutsumi S, Kamimura N, Inazawa J, Ohta T, Ichikawa H, Aburatani H, Tashiro F, et al. PH domain-only protein PHLDA3 is a p53-regulated repressor of Akt. *Cell.* 2009;136(3):535-50.
3. Miller LD, Smeds J, George J, Vega VB, Vergara L, Ploner A, Pawitan Y, Hall P, Klaar S, Liu ET, et al. An expression signature for p53 status in human breast cancer predicts mutation status, transcriptional effects, and patient survival. *Proc Natl Acad Sci U S A.* 2005;102(38):13550-5.
4. Lion M, Bisio A, Tebaldi T, De Sanctis V, Menendez D, Resnick MA, Ciribilli Y, and Inga A. Interaction between p53 and estradiol pathways in transcriptional responses to chemotherapeutics. *Cell Cycle.* 2013;12(8):1211-24.
5. Brady CA, Jiang D, Mello SS, Johnson TM, Jarvis LA, Kozak MM, Kenzelmann Broz D, Basak S, Park EJ, McLaughlin ME, et al. Distinct p53 transcriptional programs dictate acute DNA-damage responses and tumor suppression. *Cell.* 2011;145(4):571-83.
6. Tu Z, Ninos JM, Ma Z, Wang JW, Lemos MP, Desponts C, Ghansah T, Howson JM, and Kerr WG. Embryonic and hematopoietic stem cells express a novel SH2-containing inositol 5'-phosphatase isoform that partners with the Grb2 adapter protein. *Blood.* 2001;98(7):2028-38.
7. Curtis C, Shah SP, Chin SF, Turashvili G, Rueda OM, Dunning MJ, Speed D, Lynch AG, Samarajiwa S, Yuan Y, et al. The genomic and transcriptomic architecture of 2,000 breast tumours reveals novel subgroups. *Nature.* 2012;486(7403):346-52.
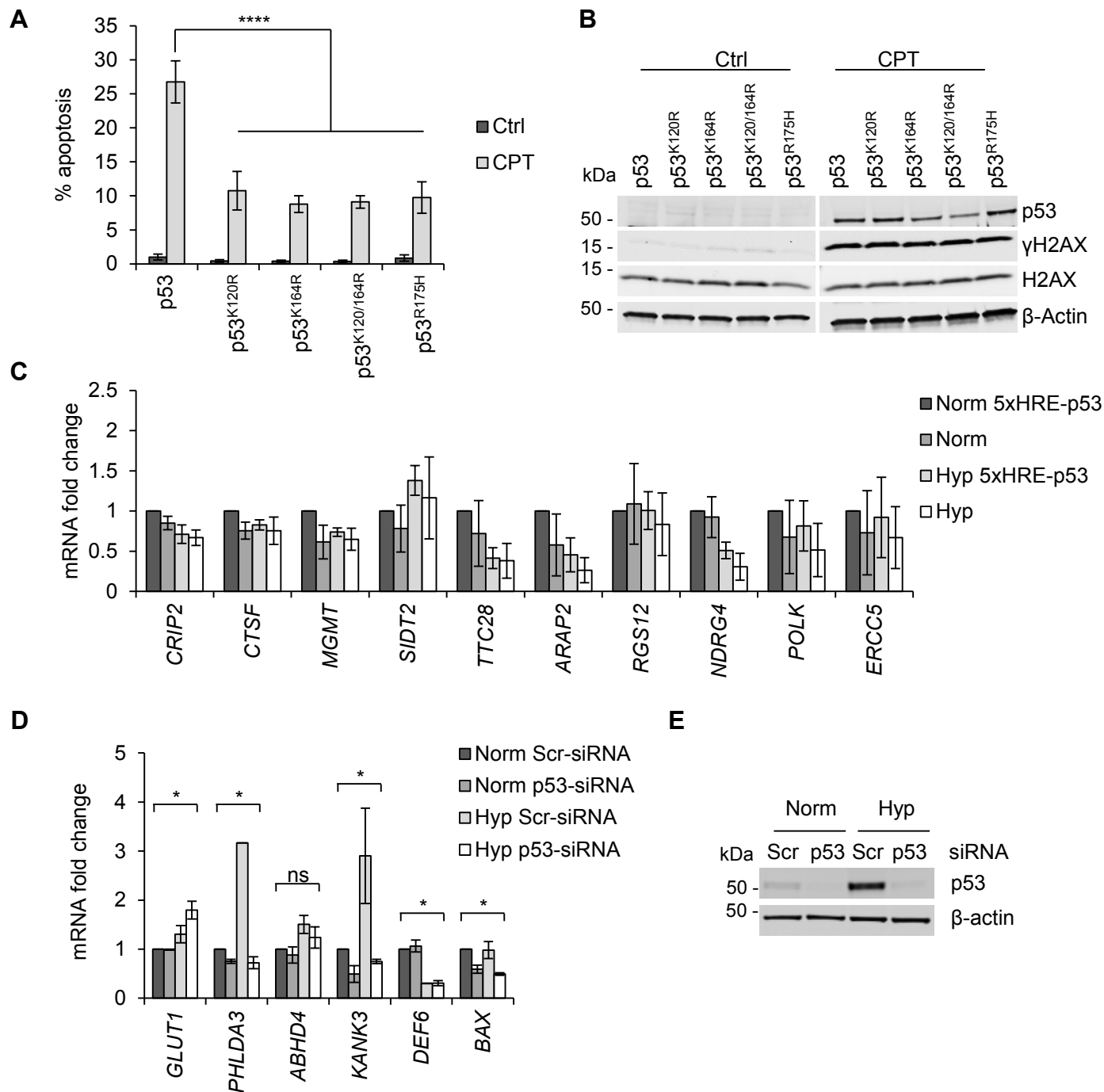
Supplemental Figure 1. Regulation of p53 and target genes in response to hypoxia

(A) Apoptosis detected morphologically in H1299 cells expressing either wt p53 (p53) or the p53 mutants (K120R, K164R, K120/164R, R175H) from the 5xHRE promoter and exposed to 16 h of 2% O_2 (to induce expression of the constructs) followed by 8 h exposure to 20 µM camptothecin (CPT) (to induce DNA damage). The bar graph shows mean $\pm$SEM (combined n=3, 2-tailed Student's t test, ****P<0.0001). **(B)** Western blotting to verify induction of p53 and DNA damage in cells from **(A)**. **(C)** qPCR testing of the hypoxic regulation of p53 target genes identified as being essential to its tumor suppressive role by Brady *et al* (5) in H1299 cells transfected with 5xHRE-p53 and exposed to 24 h of hypoxia. The remaining genes of the group of 14 are shown in Figure 1D. The bar graph shows mean $\pm$SEM (combined n=3, 2way Anova test for particular genes non-significant). **(D)** qPCR testing of the hypoxic regulation of p53 target genes in RKO cells identified by Brady *et al* (5) as being essential to p53 tumor suppressive role. Hypoxia (O_2<0.1%, Hyp), normoxia (Norm). The bar graph shows mean $\pm$SEM (combined n=3, 2way Anova test for particular genes *P<0.05, ns non-significant). **(E)** Western blotting confirming knock-down of p53 in **(D)**.
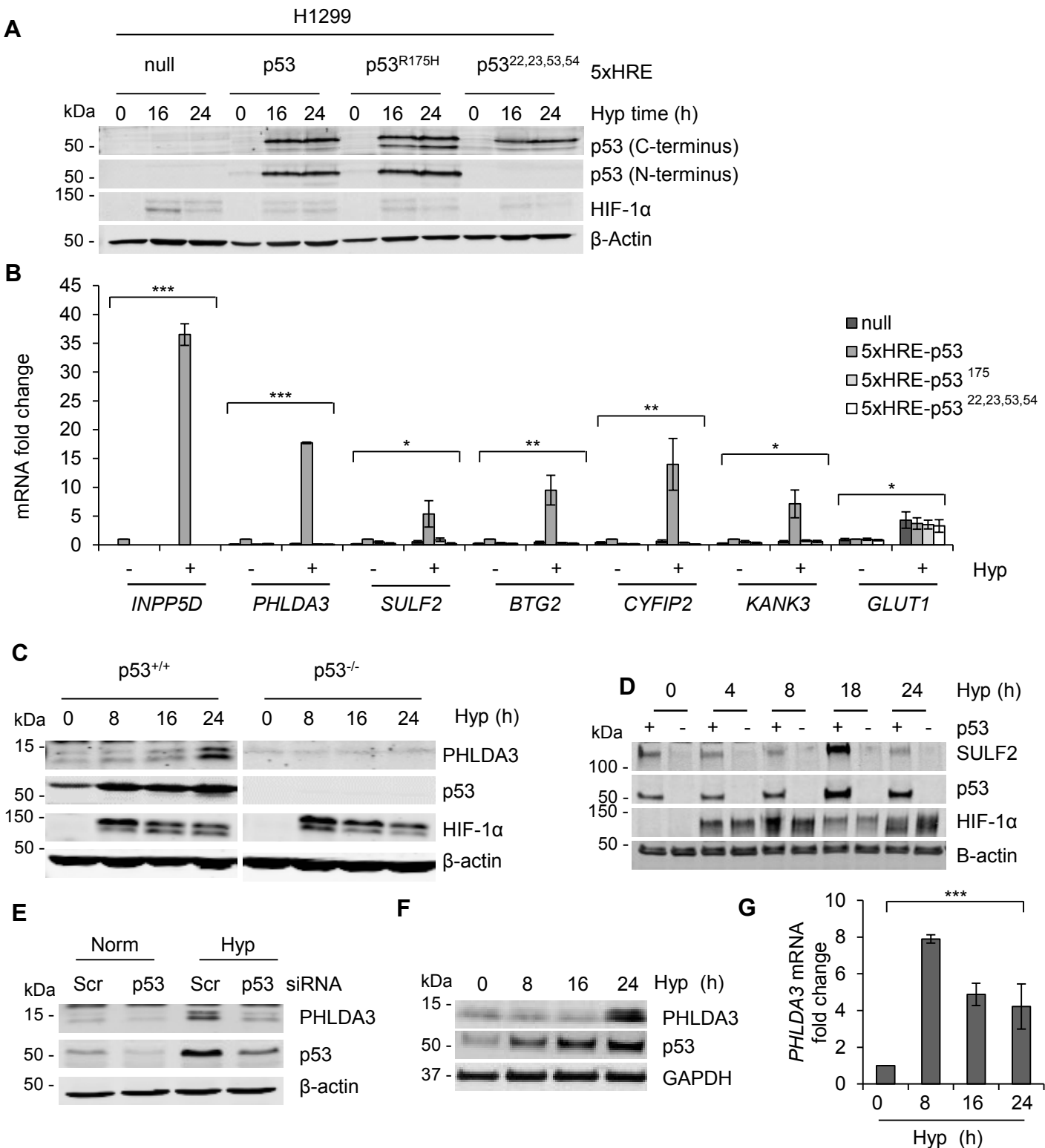
Supplemental Figure 2. Validation of the p53 targets induced in hypoxia
(A) Western blotting in H1299 cells to verify expression of p53 and mutants (p53R175H, p53²²,²³,⁵³,⁵⁴), all driven by the 5xHRE promoter, or mock-transfected (null) and exposed to 24 h hypoxia. **(B)** qPCR for p53 targets in H1299 cells from **(A)**. The bar graph shows mean ±SEM (combined n=3, 2way Anova test for particular genes *$P<0.05$, **$P<0.01$, ***$P<0.001$). **(C** and **D)** Western blotting to test expression of PHLDA3 and SULF2, respectively, in the HCT116 p53⁺/⁺ and p53⁻/⁻ pair of cell lines exposed to hypoxia for the times indicated. **(E)** Western blotting for PHLDA3 in RKO cells treated with control (Scr) or p53 siRNA and exposed 16 h of hypoxia or normoxia. **(F** and **G)** Western blotting and qPCR, respectively, for PHLDA3 in WI38 cells exposed to hypoxia for the times indicated. The bar graph shows mean ±SEM (combined n=3, 2way Anova test ***$P<0.001$).
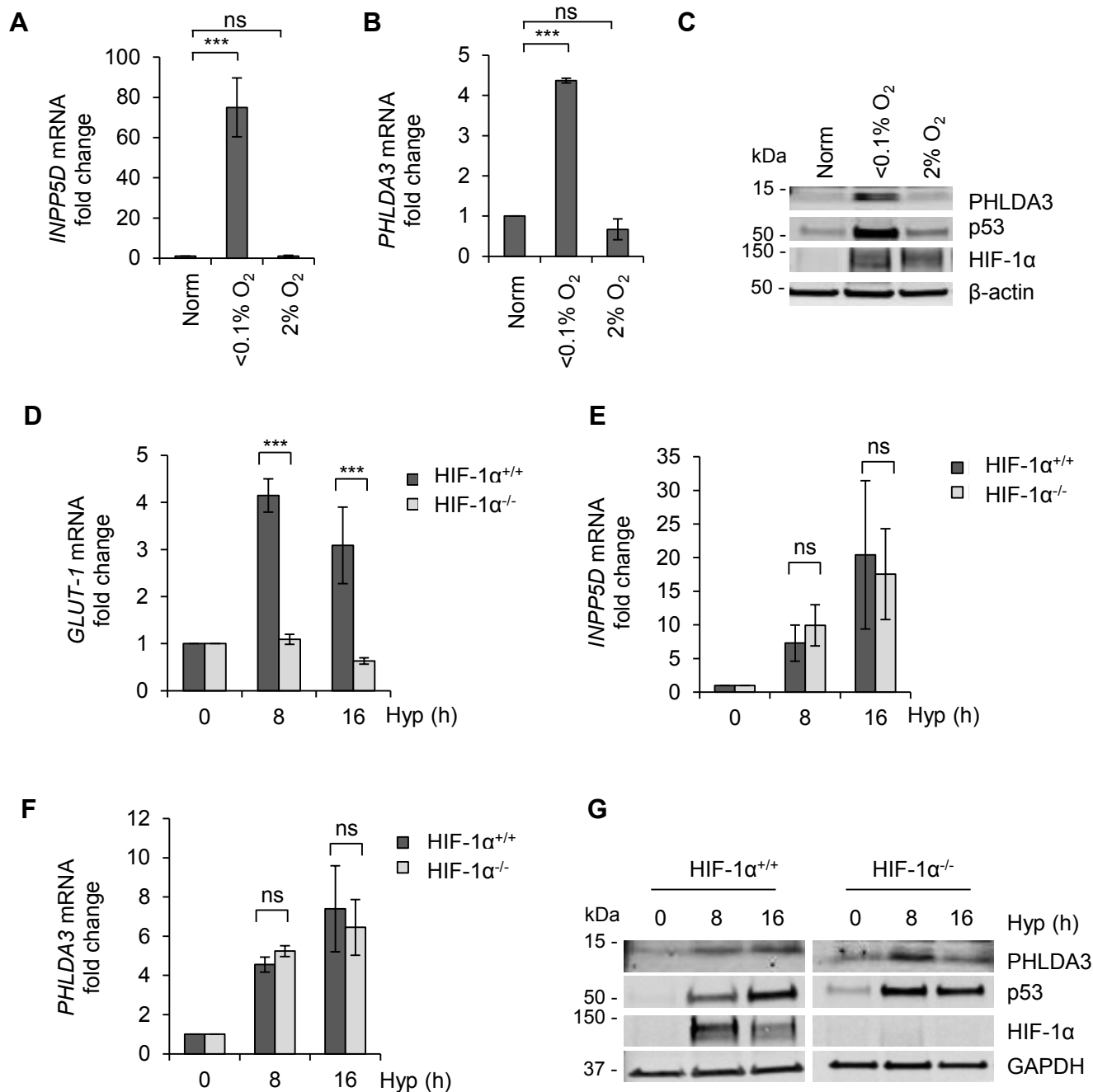
Supplemental Figure 3. p53-targets induced in hypoxia are not regulated by HIF-1α.
(A and **B)** qPCR for *INPP5D* and *PHLDA3* in RKO cells exposed to normoxia or 16 h of different hypoxia levels as indicated. (C) Western blotting for PHLDA3 on cells treated as in **(A** and **B)**. **(D-F)** qPCR for *GLUT-1*, *INPP5D* and *PHLDA3* in an isogenic pair of HIF-1α$^{+/+}$ and HIF-1α$^{-/-}$ RKO cells exposed to hypoxia for the times indicated. **(G)** Western blotting for PHLDA3 in cells treated as in **(D-F)**. All the qPCR graphs show mean $\pm$ SEM (combined n=3, 2-tailed Student's *t* tests, ***P<0.001, ns non-significant).
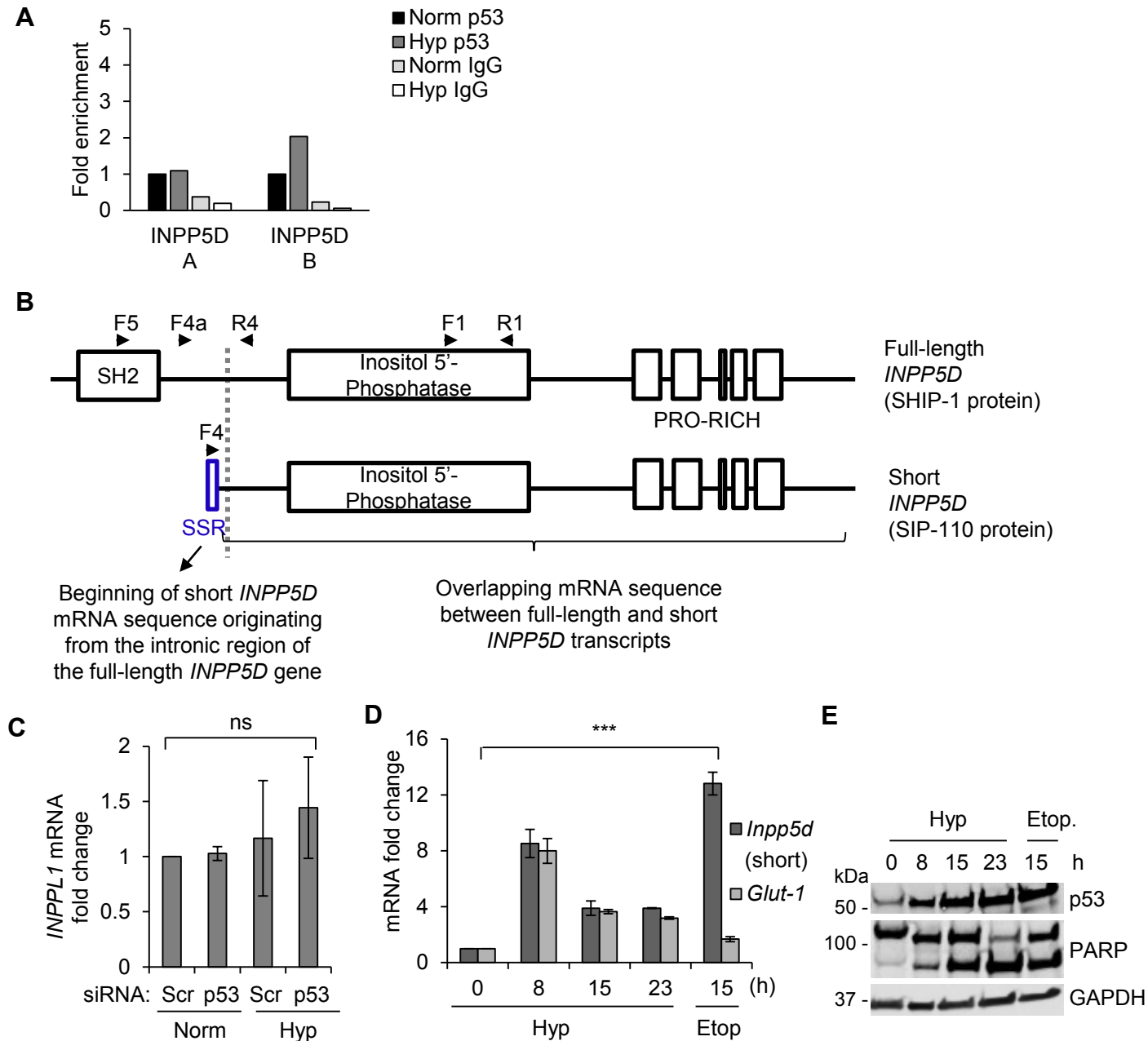
Supplemental Figure 4. p53-dependent regulation of *INPP5D* expression in hypoxia
(A) qPCR for p53 ChIP in HCT116 exposed to normoxia or 8 h of hypoxia for the two p53-RE at the INPP5D locus identified in (4) and referred as "A" and "B" (bars show mean of triplicate values, n=1). **(B)** A schematic organization of *INPP5D* transcripts. The full-length *INPP5D* transcript encodes for the SHIP-1 protein containing the N-terminal Src-homology 2 (SH2) domain, the central phosphatase domain and the proline-rich region towards the C-terminus. The short *INPP5D* transcript is transcribed from the internal promoter localized in the intronic region spanning Exons 5 and 6 of the full-length *INPP5D* (6). The short *INPP5D* transcript encodes the SIP-110 protein and includes the stem-SHIP-region (SSR) originating from the intronic sequence, which is followed by exon 6 of the full-length transcript and contains exact downstream sequence as the full-length *INPP5D*/SHIP-1 (6). Arrows indicate localization of primers used in Figure 2C. **(C)** qPCR for *INPPL1* gene encoding SHIP2 protein in RKO cells from Supplemental Figure 2E. **(D)** qPCR for short *INPP5D* and Glut-1 in mouse embryonic stem cells (CCE line) exposed to hypoxia or Etoposide (Etop). The qPCR bar graphs show mean $\pm$SEM (combined n=3, 2way Anova test ***P<0.001, ns non-significant). **(E)** Western blotting with indicated antibodies in cells from **(D).**

A

Fold change

Cancers:	PHLDA3	INPP5D	SULF2	BTG2	CYFIP2	KANK3	Mutation:
Brain and CNS Cancer Cell Line (G.)							*TP53* (m.)
Multi-cancer Cell Line (G.)							*TP53* (m.)
Kidney Cancer Cell Line (G.)							*TP53* (m.)
Colorectal Cancer Cell Line (G.)							*TP53* (m.)
Bladder Cancer Cell Line (G.)							*TP53* (m.)
Breast Cancer Cell Line (G.)							*TP53* (m.)
Breast Cancer Cell Line (N.)							*TP53* (m.)
Kidney Cancer Cell Line (C.)							*TP53* (m.)
Melanoma Cell Line (J.)							*TP53* (m.)
Hepatocellular Carcinoma (C. L.)							*CTNNB1* (m.)
Prostate Carcinoma Metastasis (G. P.)							*ETS* family (g. f.)
Prostate Carcinoma Metastasis (G. P.)							*ETS2* (d.)
Prostate Carcinoma Metastasis (G. P.)							*ERG* (r.)
Bladder Cancer Cell Line (G.)							*RB1* (m.)
Brain and CNS Cancer Cell Line (G.)							*RB1* (m.)
Breast Cancer Cell Line (G.)							*CDKN2A* (m.)
Leukemia Cell Line (G.)							*PTEN* (m.)
Lung Cancer Cell Line (G.)							*EGFR* (m.)
Breast Cancer Cell Line (G.)							*MAP2K4* (m.)
Ovarian Serous Adenocarcinoma (A. O.)							*KRAS* (m.)
Acute Myeloid Leukemia (W. L.)							*NRAS* (m.)
B-Cell Acute Lymphoblastic Leukemia (Bh. L.)							*TCF3-PBX1* (g. f.)
Childhood Acute Myeloid Leukemia (Ba. L.)							*CBFB-MYH11* (g. f.)

Fold change legend:
>4, 3, 2, 1, -1, -2, -3, -4, <-5, ns, nt

B

Cancers:	PUMA	BID	PERP	BAX	PIG3	NOXA	Mutation:
Sarcoma Cell Line (G.)							*TP53* (m.)
Multi-cancer Cell Line (G.)							*TP53* (m.)
Melanoma Cell Line (J.)							*TP53* (m.)
B-Cell Childhood Acute Lymph. Leukemia (K. L.)							11q23 *MLL* (r.)
Acute Lymphoblastic Leukemia (A. L.)							*ETV6-RUNX1* (g. f.)
Acute Myeloid Leukemia (W. L.)							*NPM1* (m.)
Acute Myeloid Leukemia (H. L.)							11q23 *MLL* (r.)
Myxoid/Round Cell Liposarcoma (B. S.)							*PIK3CA* (m.)
Multi-cancer Cell Line (G.)							*BRCA2* (m.)
Multi-cancer Cell Line (G.)							*CTNNB1* (m.)
Multi-cancer Cell Line (G.)							*APC* (m.)
Lung Adenocarcinoma (B. L.)							*KRAS* (m.)
Brain and CNS Cancer Cell Line (G.)							*BRAF* (m.)
Borderline Ovarian Serous Neoplasm (S. O.)							*BRAF* (m.)

C

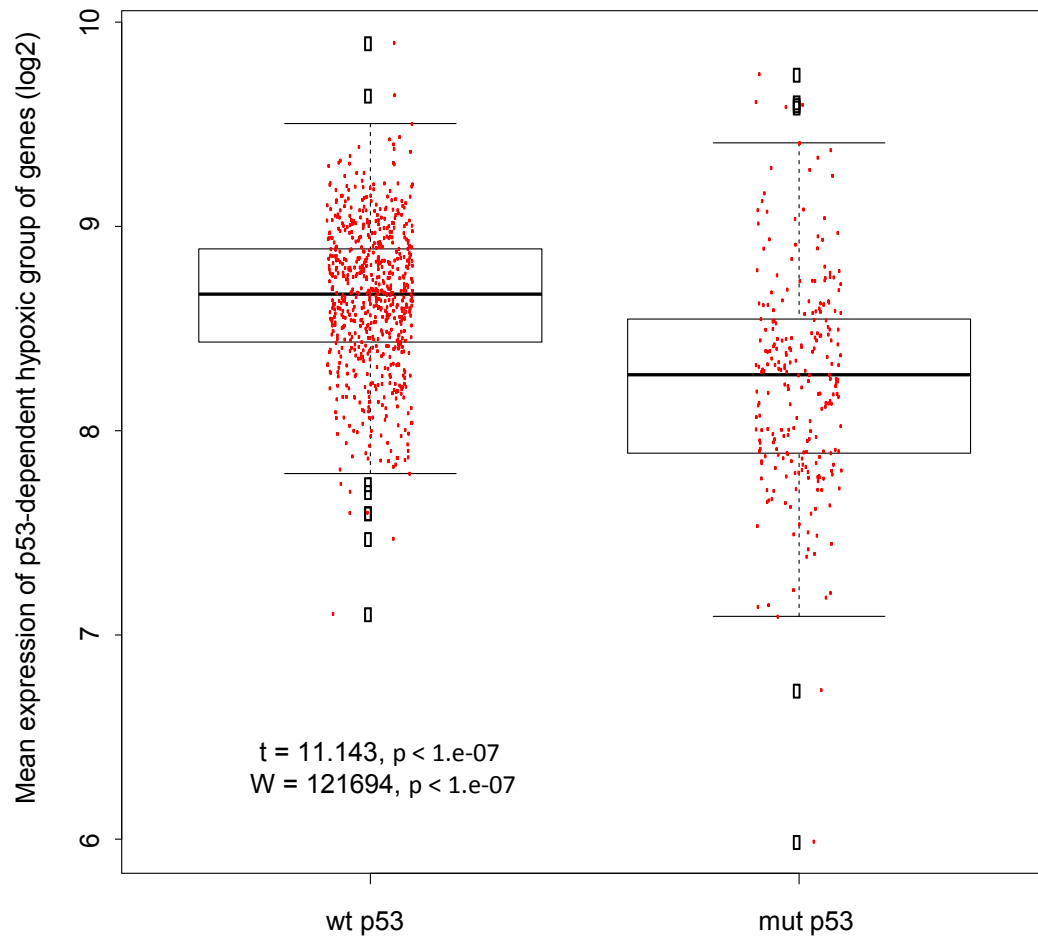| Cancers:	PUMA	BID	PERP	BAX	PIG3	NOXA	Outcome:
Anaplastic Oligodendroglioma (N. B.)							Dead at 1 Year
Prostate Carcinoma (S. P.)							Dead at 1 Year
Lung Adenocarcinoma (B. L.)							Dead at 3 Years
Lung Adenocarcinoma (D. L.)							Dead at 3 Years

Supplemental Figure 5. Oncomine analysis of hypoxia-inducible p53 targets versus DNA damage-inducible p53 targets in publically available datasets.
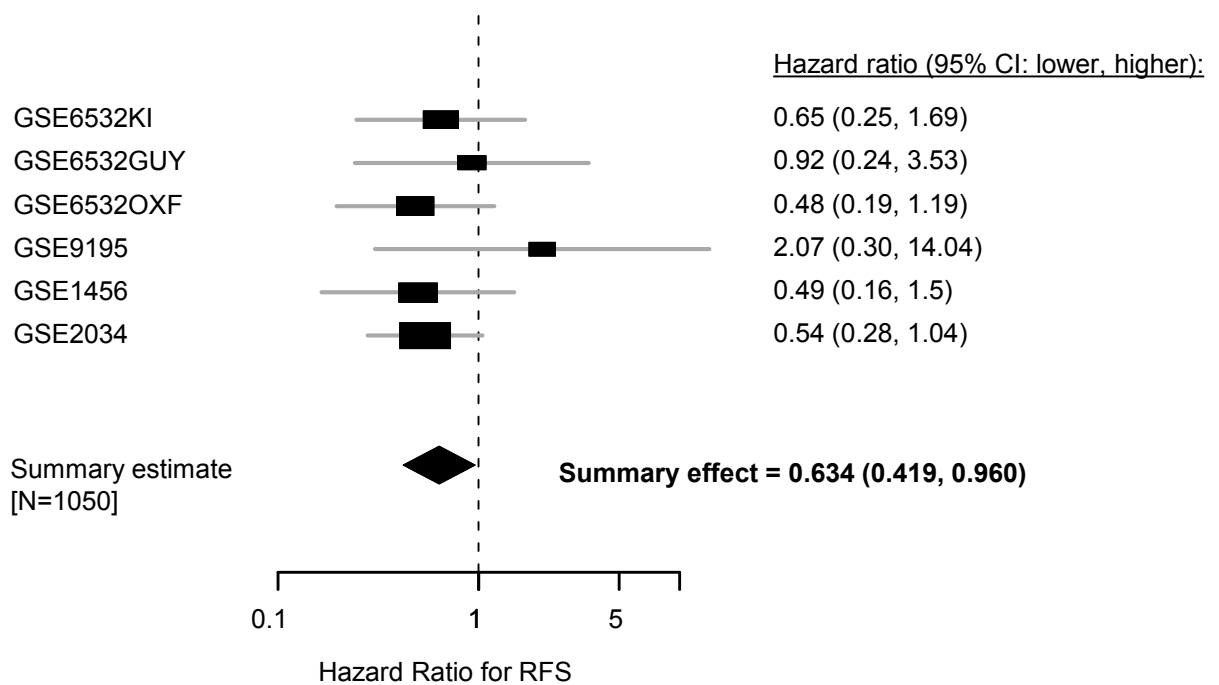
(A) The heatmap showing mutational analysis of hypoxia-inducible p53 targets as a group of genes (*PHLDA3, INPP5D, SULF2, BTG2, CYFIP2* and *KANK3*) performed using the Oncomine database (www.oncomine.com; Oncomine 4.4.3 research edition). Every row in the heatmap represents a single experiment that was significantly associated with the tested group of genes in the Oncomine database out of all available datasets. On the left side is reported a cancer type and the Oncomine database reference in the brackets. On the right side is stated a gene mutation which was significantly correlated with expression of analyzed group of genes. The threshold criteria used for the analysis were as follows: odds ratio 2.0, p-value 0.01, mRNA as a data type, top 10% of over- or under-expressed genes. The significant ($p \leq 0.05$) up- or down-regulation of genes as a fold change was marked in red and blue (respectively) in every experiment. Not significant (ns) or not tested (nt) expression of genes in particular experiments is coded in white and grey, respectively. Dashed-line box highlights datasets that refer to p53 mutational status. Enrichment in p53 mutation with respect to all mutations reported by Oncomine (N=185 datasets with characterized mutation status) was significant (hypergeometric test, p=0.0279). **(B)** The heatmap generated using the same method and criteria as in **(A)** but for the known DNA damage-inducible p53 targets as a group of genes (*PUMA, BID, PERP, BAX, PIG3, NOXA*). Dashed-line box highlights datasets that refer to p53 mutational status. Enrichment in p53 mutation with respect to all mutations reported by Oncomine was not significant (hypergeometric test , p=0.599). **(C)** The heat map showing a grouped expression of known DNA damage-inducible pro-apoptotic p53 targets (*PUMA, BID, PERP, BAX, PIG3, NOXA*) correlated with a clinical outcome in cancer patients tested against all available datasets in the Oncomine database. Abbreviations: Garnett CellLine (G.), Neve CellLine (N.), Compendia CellLine (C.), Johansson CellLine (J.), Chiang Liver (C. L.), Grasso Prostate (G. P.), Anglesio Ovarian (A. O.), Wouters Leukemia (W. L.), Bhojwanie Leukemia 2 (Bh. L.), Balgobind Leukemia (Ba. L.), Kang Leukemia (K. L.), Armstrong Leukemia (A. L.), Haferlach Leukemia (H. L.), Barretina Sarcoma (B. S.), Bild Lung (B. L.), Sieben Ovarian (S. O.), Nutt Brain (N. B.), Setlur Prostate (S. P.), Bild Lung (B. L.), DirectorsChallenge Lung (D. L.), mutation (m.), gene fusion (g. f.), deletion (d.), rearrangement (r.).

## p53 status vs p53-dependent hypoxic group of genes

t = 11.143, p < 1.e-07
W = 121694, p < 1.e-07

B

	Hazard ratio (95% CI: lower, higher):
GSE6532KI	0.65 (0.25, 1.69)
GSE6532GUY	0.92 (0.24, 3.53)
GSE6532OXF	0.48 (0.19, 1.19)
GSE9195	2.07 (0.30, 14.04)
GSE1456	0.49 (0.16, 1.5)
GSE2034	0.54 (0.28, 1.04)

Summary estimate
[N=1050]

Summary effect = 0.634 (0.419, 0.960)

Hazard Ratio for RFS

Supplemental Figure 6. Expression of a p53-dependent hypoxia-inducible group of genes is repressed in p53 mutant breast cancer cases.

(A) Boxplots showing the summary expression distribution for the p53-depedent hypoxia signature (namely the genes: *PHLDA3, INPP5D, SULF2, BTG2, CYFIP2* and *KANK3*) in p53 wild-type (WT) and mutants (mut) breast cancer samples. Median, first and 3rd quartiles, and range are shown. The mean expression of these genes was considered as the summary expression, similar results were obtained when using the median expression. Red dots correspond to the summary expression level in single samples. T-test and Wilcoxon test results are provided on the plot. A published p53 signature in breast cancer was used to infer p53 status (3). The p53 prediction algorithm was implemented following the methods provided in the original publication, including pre-processing. Six curated retrospective breast cancer datasets deposited in the GEO repository (GSE6532KI, GSE6532GUY, GSE6532OXF, GSE9195, GSE1456 and GSE2034) were used. Batch effects were minimized by using the inSilicoMerging function with ComBat correction option (http://www.bioconductor.org/packages/2.12/bioc/html/inSilicoMerging.html). **(B)** A Forest plot showing meta-analysis on 6 curated retrospective breast cancer datasets from A on the group of genes (*PHLDA3, INPP5D, SULF2, BTG2, CYFIP2* and *KANK3)*. Hazard-ratio (HR) for recurrence-free survival (RFS) (high expression levels associated with good prognosis if HR<1, worse prognosis if HR>1), with 95% confidence interval, is shown for each datasets and for the summary effect on the 1050 samples.

A
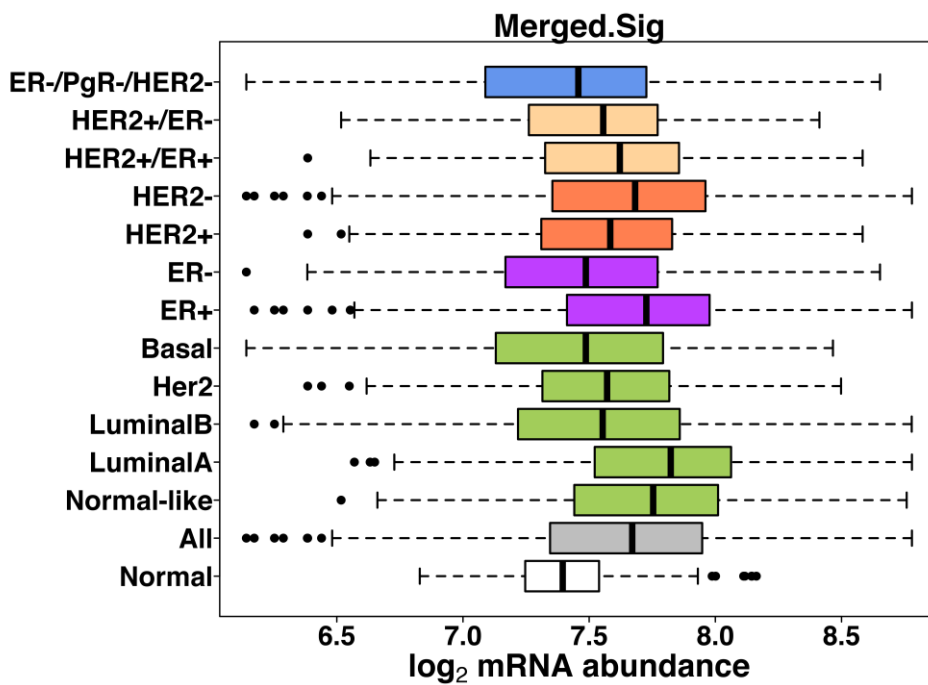
B

	Significance level
ANOVA	6.46E-49
Post-hoc pairwise comparison	**Significance level (Adjusted P)**
Her2 vs Basal	0.062
LuminalA vs Basal	6.46E-11
LuminalB vs Basal	0.094
Normal vs Basal	0.877
Normal-like vs Basal	6.68E-11
LuminalA vs Her2	6.55E-11
LuminalB vs Her2	0.989
Normal vs Her2	0.013
Normal-like vs Her2	0.0001
LuminalB vs LuminalA	6.47E-11
Normal vs LuminalA	6.47E-11
Normal-like vs LuminalA	0.532
Normal vs LuminalB	0.022
Normal-like vs LuminalB	1.71E-07
Normal-like vs Normal	8.81E-11

Supplemental Figure 7. Expression of a p53-dependent hypoxia-inducible group of genes in subtypes of breast cancer.
(A) Expression of p53-dependent hypoxia-inducible group of genes (Merged.Sig) in normal breast tissues (Normal) and breast cancer subtypes using METABRIC cohort; boxplots showing median, first and third quartiles, extremes and outliers. Expression for the group of genes is summarized as median expression. The subtype categorizations are described in Curtis *et al*. (7). **(B)** Results for the ANOVA analysis using expression in normal breast (white boxplot) and PAM50 subtypes (green boxplots). Post-hoc pairwise comparisons following ANOVA were performed using Tukey's HSD test.
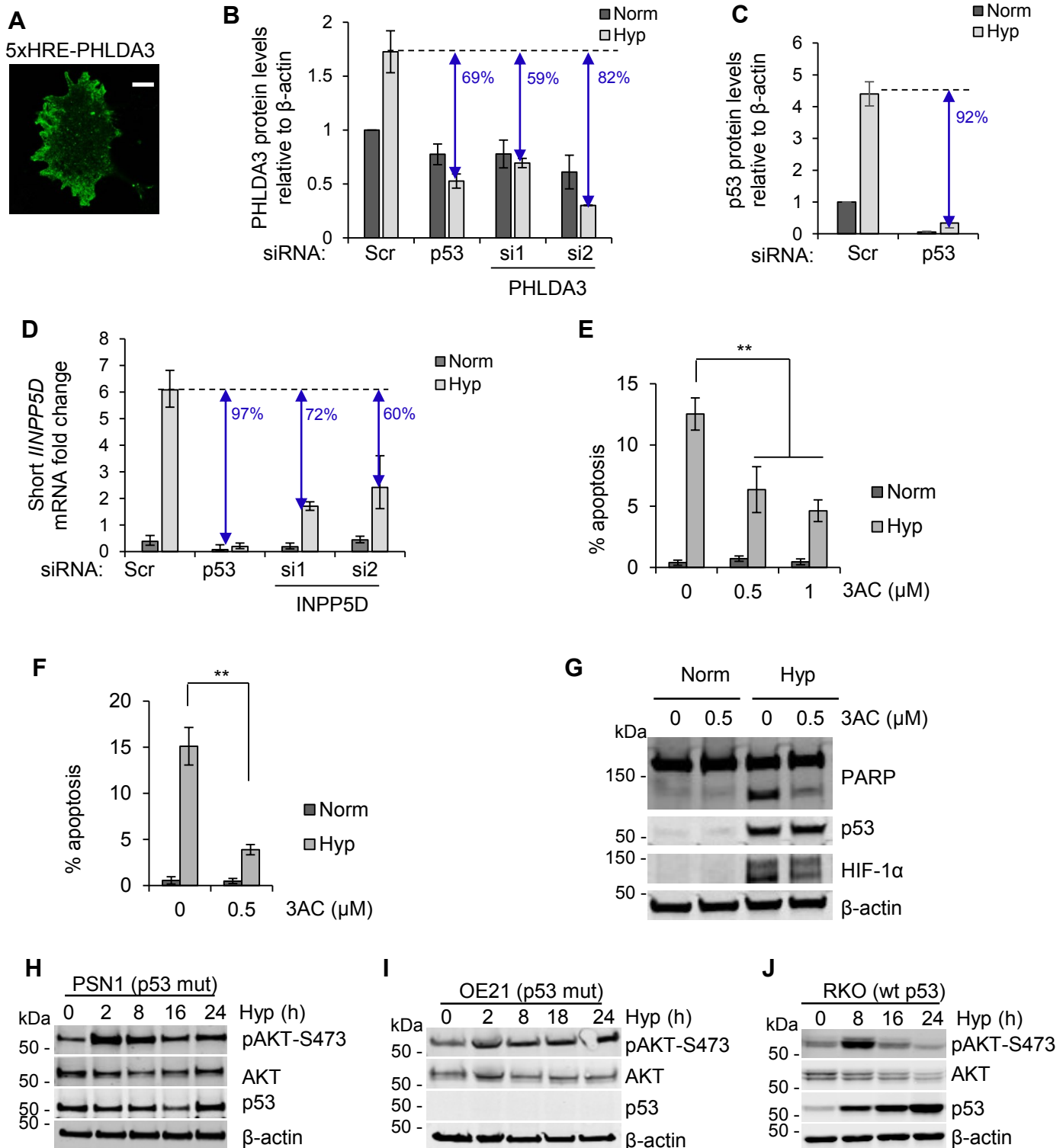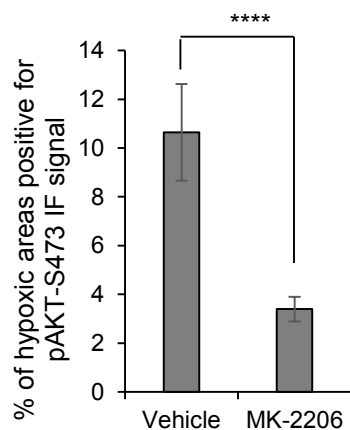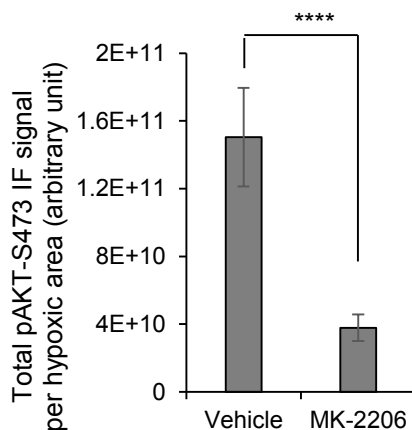
Supplemental Figure 8. Regulation of pAKT and apoptosis by p53 and the targets PHLDA3 and SHIP-1/*INPP5D* in hypoxia.

(A) Immunofluorescent staining of 5xHRE-PHLDA3 transfected in H1299 cells and exposed to 24 h of hypoxia. Scale bar 10 μm. (B and C) A bar graph showing quantitation of an avarage PHLDA3 and p53 siRNA knock-downs, respectively, quantified from western blotting (relative to β-actin); n=3. % of knock-down efficiency compared to Scr-siRNA is indicated on the graphs with a blue arrow. **(D)** Representative qPCR for short *INPP5D* in RKO cells treated with Scr, INPP5D or p53 siRNA as indicated and exposed to normoxia or 14 h of hypoxia. % of knock-down efficiency compared to Scr-siRNA is indicated on the graph with a blue arrow. **(E** and **F)** Apoptosis detected morphologically in HCT116 and RKO cells, respectively, exposed to normoxia or 18 h of hypoxia in the presence or absence of a SHIP-1 inhibitor, 3AC. **(G)** Apoptosis in cells from **(F)** detected additionally by PARP cleavage. **(H-J)** Western blotting comparing AKT-S473 phosphorylation in PSN1, OE21 and RKO cells, respectively, exposed to hypoxia for the times indicated.
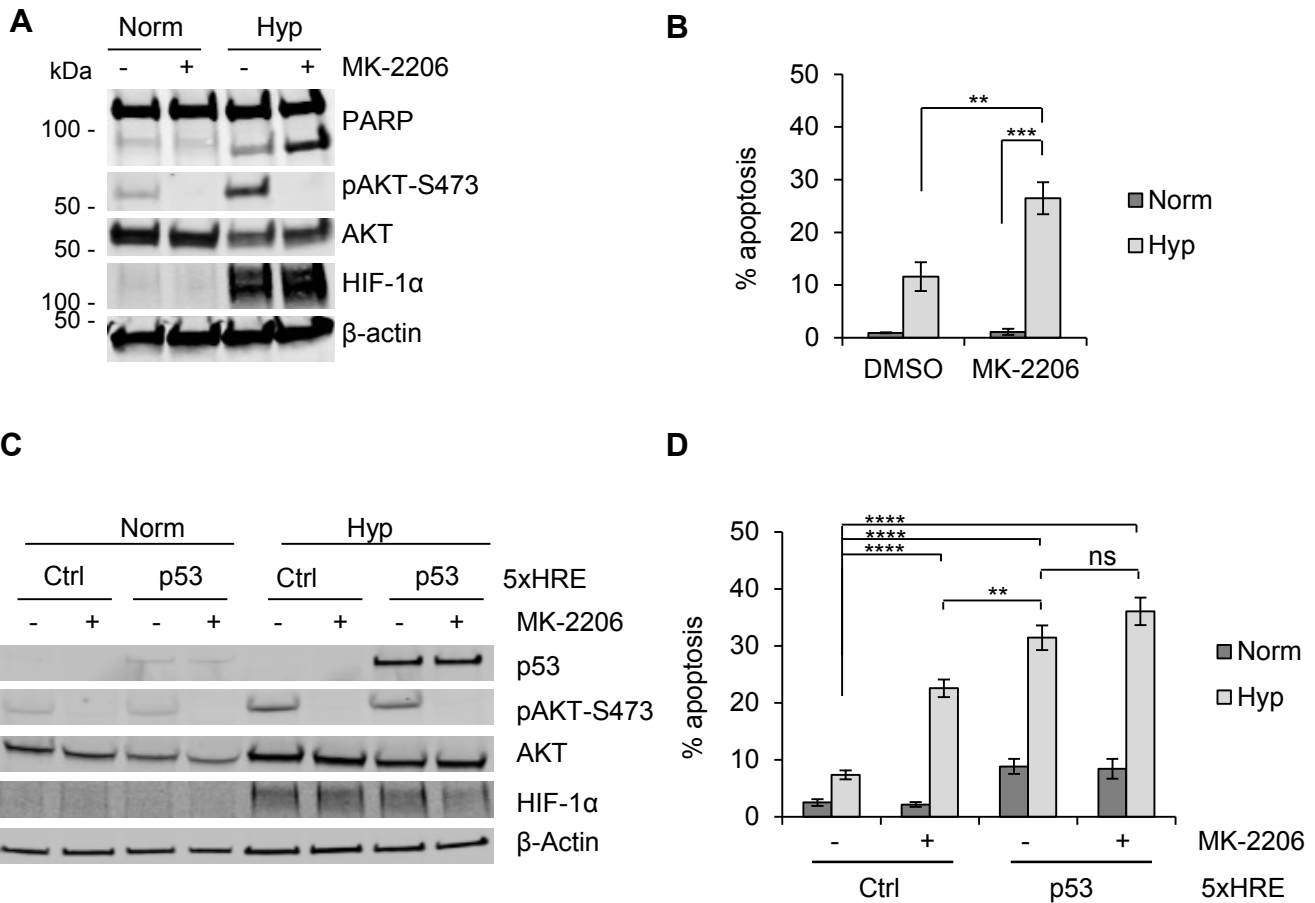
Supplemental Figure 9. Apoptosis induced by inhibition of AKT with MK-2206.
(A and **B)** Apoptosis detected by PARP cleavage or morphologically in PSN1 cells treated with MK-2206 or DMSO and exposed to 20 h of hypoxia or normoxia. The bar graph shows mean ±SEM (n=3, 2-tailed Student's *t* tests (***P<0.001; **P<0.01). **(C** and **D)** Apoptosis detected by PARP cleavage or morphologically, respectively in H1299 transfected either with 5xHRE-p53 or Ctrl and exposed to 16 h of hypoxia or normoxia in the presence of DMSO or MK-2206. The bar graph shows mean ±SEM (n=3, 2way Anova test (****P<0.0001) followed by 2-tailed Student's *t* tests (****P<0.0001; **P<0.01, ns non-significant).
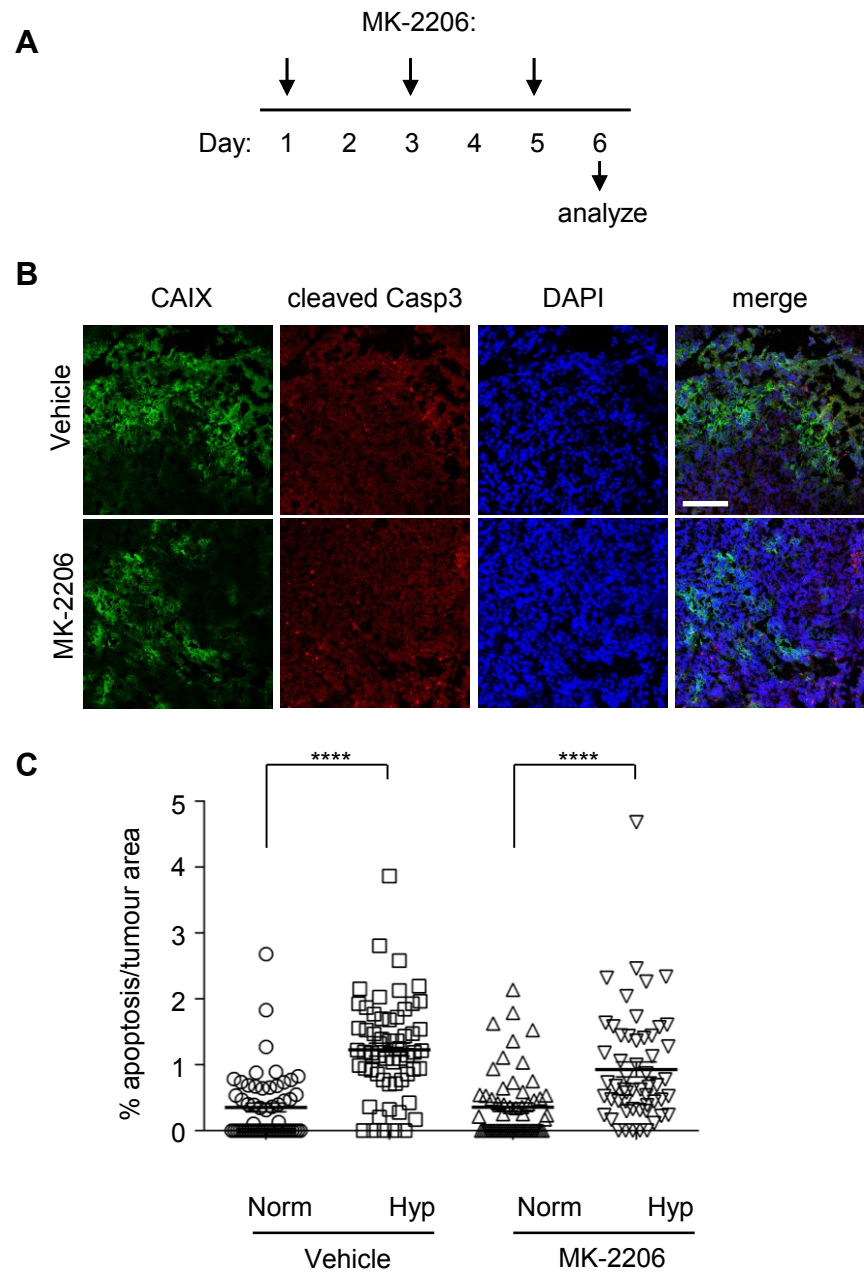
A

B

Supplemental Figure 10. Quntitation of pAKT-S473 localization in hypoxic areas in OE21 xenografts treated with MK-2206.
(A) Mice were given a vehicle or 60 mg/kg MK-2206 on three alternate days and 24 h after last dose tumors were collected for IF analysis. Hypoxic areas were visualized with pimonidazole and active AKT with pAKT-S473 staining, respectively, as shown in representative images in Figure 7B. The bar graph shows mean ± SEM of % hypoxic areas positive for pAKT-S473 staining. **(B)** The bar graph shows mean ± SEM of pAKT-S473 IF signal per hypoxic area. For both graphs 40 hypoxic areas were analyzed for Vehicle and 33 hypoxic areas for MK-2206, from 3 animals per each treatment group (2-tailed Student's *t* tests: ****$P<0.0001$).
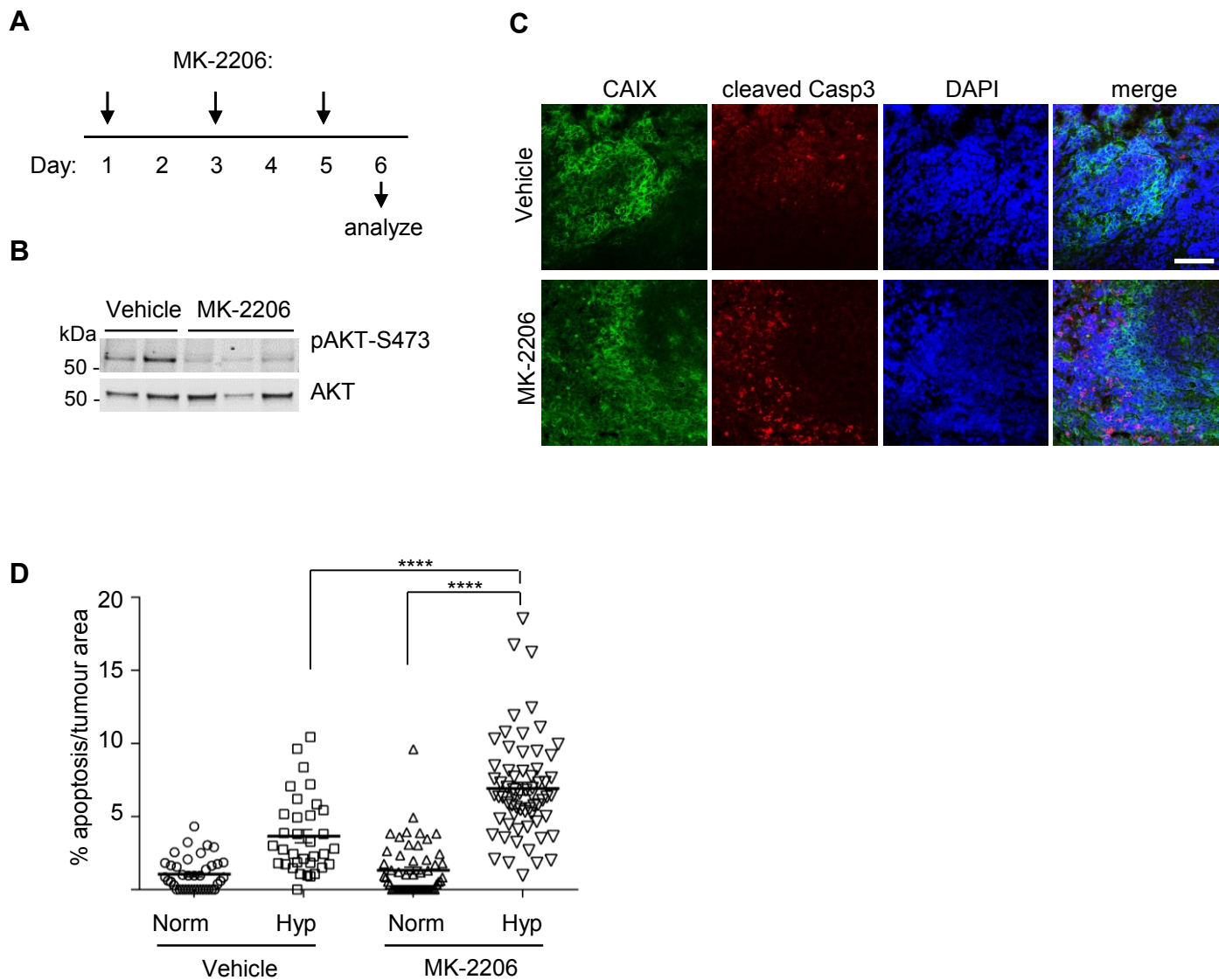
Supplemental Figure 11. Inhibition of AKT with MK-2206 *in vivo* in p53-deficient PSN1 tumors.
(A) A schematic of MK-2206 treatment in PSN1 xenografts; Mice were given a vehicle or 60 mg/kg MK-2206 on three alternate days and 24 h after last dose tumors were collected for IF analysis. **(B)** Western blotting showing pAKT-S473 inhibition in tumors from **(A)**. **(C)** Representative images of co-localization of cleaved Caspase 3 with hypoxic areas stained with CAIX antibody. Scale bar 100 μm **(D)** Plots are showing percentage of apoptosis per either normoxic or hypoxic regions from all the regions analyzed overlaid with mean ± SEM from 3 animals per each group (2-tailed Student's *t* tests; ****P<0.0001).

A

MK-2206:

Day: 1 2 3 4 5 6

analyze

B

C

Supplemental Figure 12. Inhibition of AKT with MK-2206 *in vivo* in p53 wt HCT116 tumors.
(A) A schematic of MK-2206 treatment in HCT116 xenografts; Mice were given a vehicle or 60 mg/kg MK-2206 on three alternate days and 24 h after last dose tumors were collected for IF analysis. **(B)** Representative images of co-localization of cleaved Caspase 3 with hypoxic areas stained with CAIX antibody. Scale bar 100 μm **(C)** Plots are showing percentage of apoptosis per either normoxic or hypoxic regions from all the regions analyzed overlaid with mean ± SEM from 3 animals per each group (2-tailed Student's *t* tests; ****P<0.0001).